12

Photogrammetry and remote sensing in support of GDI

Gottfried Konecny

12.1 Introduction

As the largest cost in a GDI is arguably that of building and maintaining the databases, an overview of two major geospatial data acquisition technologies is presented here. The technologies and their platforms are introduced in Sections 12.2 to 12.4, and the data acquisition techniques for vector and raster data are described in Sections 12.5 and 12.6. The acquisition of digital terrain models is discussed in Section 12.7, and thematic data acquisition from different platforms in Section 12.8. Parcel-based data systems are of particular significance to a large variety of civic applications, both in urban and in rural areas. The parcel database and the database of administrative areas derived from it form an integral part of the foundation data in the GDI. The role of photogrammetry and remote sensing in building and maintaining these parcel-based systems is presented in Section 12.9. Data acquisition decisions are usually a balance between cost, required accuracy, and timeliness. Hence, the cost–performance of various photogrammetric and remote sensing products are compared in Section 12.10.

12.2 Remote sensing and photogrammetry

Remote sensing is a technique for obtaining information about distant objects without direct contact. The information is obtained from the object's reflections of force fields by sensors that react to electromagnetic radiation spatially separating the reflections. The directional separation of the reflections permits us to accumulate the signals in the form of images. In the visual spectrum, these have been generated for 150 years by lens objectives on to an image plane and fixed on photographic emulsions. Today, they can be accumulated by digitally separated signals as image pixels. The images can be used directly for image
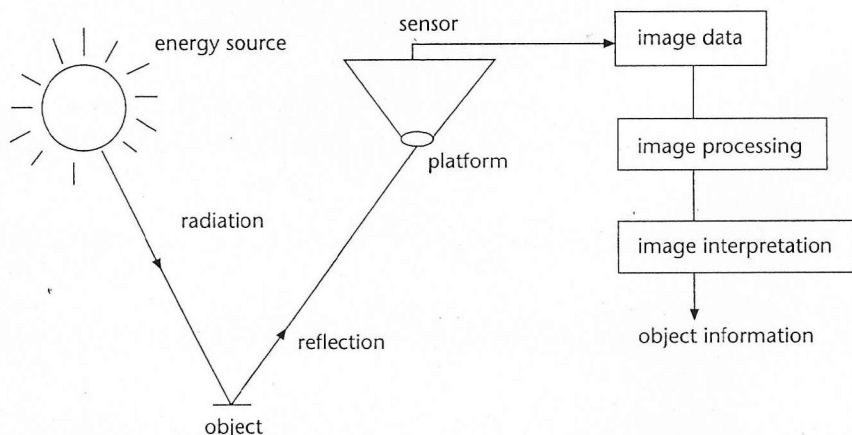
FIGURE 12.1 Principles of remote sensing.

interpretation so that objects can be detected, recognized, and classified (Figure 12.1).

In photogrammetry two different images are taken from different viewing stations to make a 3D geometric model of the image objects. The process of reconstructing these objects geometrically, based on accurate measurements made in the images, is called photogrammetry. This is therefore a special application of remote sensing (Figure 12.2).

12.3 Geospatial data infrastructure in relation to photogrammetry and remote sensing

Geospatial information systems offer the possibility of generating a digital geometric and semantic model of an object. Objects cover the Earth's surface, and since knowledge of the object distribution on the Earth's surface is essential for planning, managing, and monitoring the natural and human environment, spatial information systems are of great scientific, technical, and economic importance.

A modern geospatial information system is based on the alternative technologies available to geoinformatics (or geomatics) which are described in this book. It employs hardware and software for input, manipulation, storage, and output of digital data for user-specified spatial information products. The data in raster, vector, and alphanumeric form constitute the most costly, and thus most important, component of the system (Figure 12.3). The system must also contain an administrative component stressing the purpose and the application (Figure 12.4). The three major components of a system are the hardware and software, data, and administration, consuming approximately 10 per cent, 80 per cent, and 10 per cent of the total effort (see, for example, Dangermond, 1997).
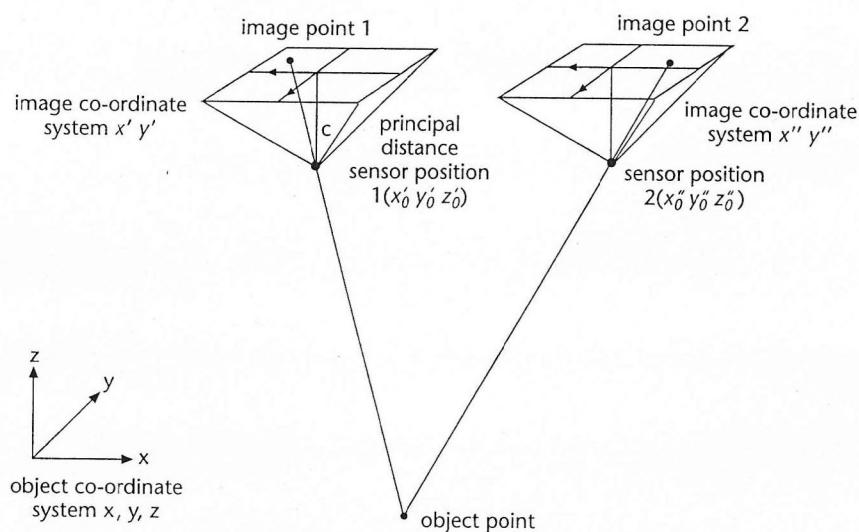
$$x' = -c\,\frac{a'_{11}(x - x'_0) + a'_{12}(y - y'_0) + a'_{13}(z - z'_0)}{a'_{31}(x - x'_0) + a'_{32}(y - y'_0) + a'_{33}(z - z'_0)}$$

$$y' = -c\,\frac{a'_{21}(x - x'_0) + a'_{22}(y - y'_0) + a'_{23}(z - z'_0)}{a'_{31}(x - x'_0) + a'_{32}(y - y'_0) + a'_{33}(z - z'_0)}$$

These equations are called collinearity equations.
$a_{11}, a_{12} \ldots a_{33}$ are the coefficients of a three-dimensional orthogonal rotation matrix representing the direction cosines of the space angles between the relative axes.

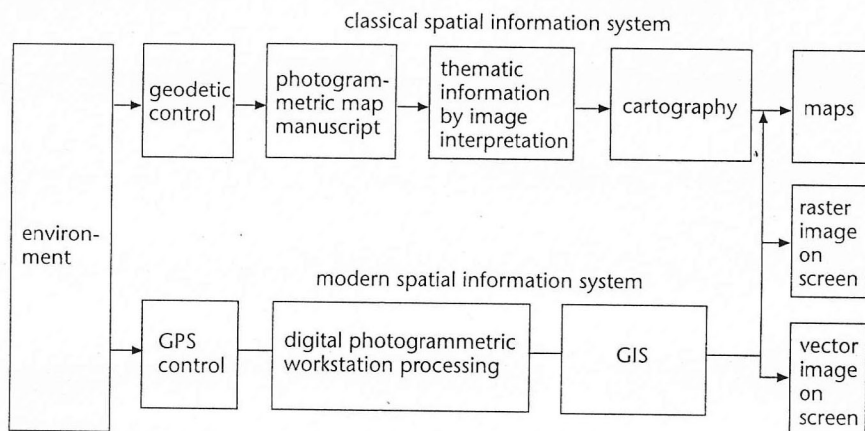FIGURE 12.2 Principles of photogrammetry.

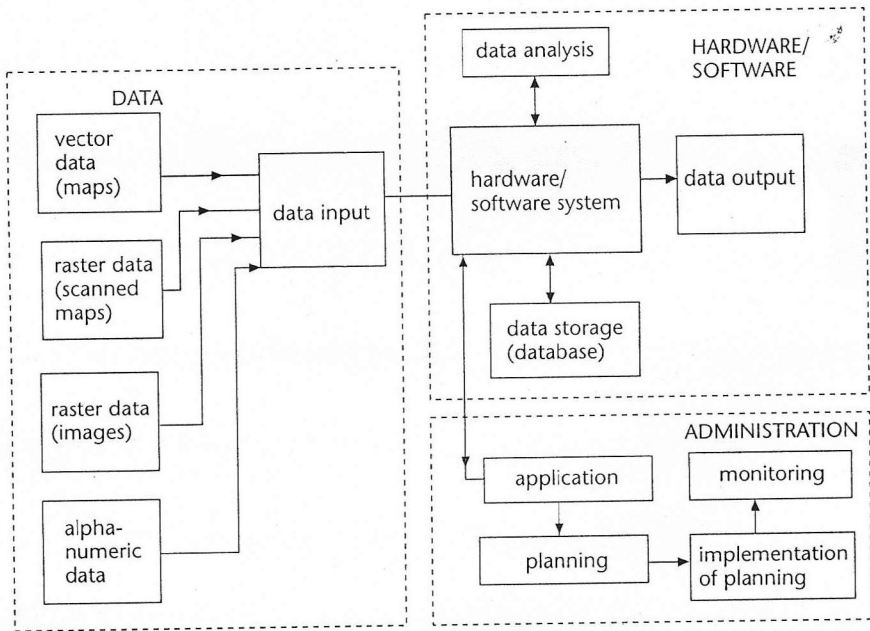FIGURE 12.3 Classical and modern geospatial information system.

FIGURE 12.4 Components of a modern geospatial information system.

These systems are extensively applied to routinely produce data, which can be made accessible through the GDI architectures presented in Chapter 9. To control the contribution to the overall cost, the data to be surveyed need to be carefully defined using the techniques described in Chapter 10, for example.

12.4 Sensors and platforms

The classic tool for remote sensing is the aerial survey camera. It was invented in 1916 by Messter and consists of an optical system optimized for high resolution and for minimum distortion (Figure 12.5). The compensation of imaging errors occurs via lens elements with different refraction indices. The minimal distortion $d\tau$ is selected with respect to the principal point, forming the origin of the image co-ordinate system. It is marked during factory calibration by fiducial marks whose intersection defines the principal point. All co-ordinate conversions and photogrammetric computations (space intersections, space resections) are referred to the image co-ordinate systems marked by the principal points.

To maintain geometric precision of the exposed film, the film is kept flat by a vacuum pressure plate during exposure. The camera's mechanism permits successive exposures at intervals of two to three seconds, during which the camera must transport the film, apply the vacuum to the pressure plate, and perform the exposure lasting from 1/100th to 1/1000th of a second. The successive expo-
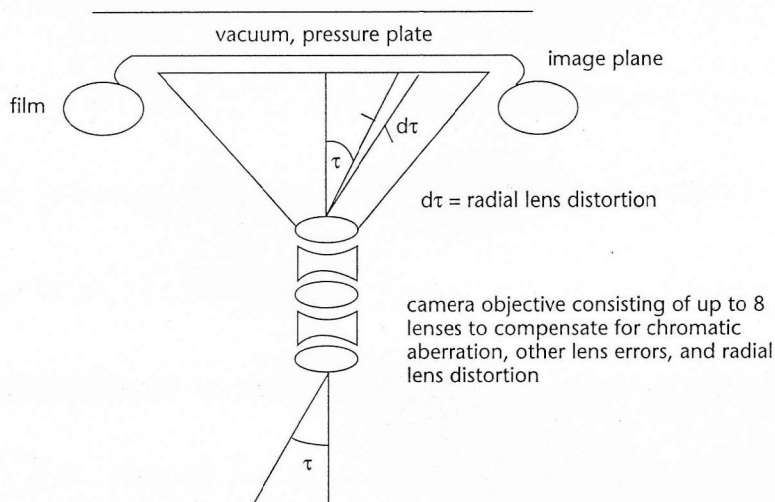
FIGURE 12.5 Aerial survey camera.

sures must overlap by at least 60 per cent to permit stereo coverage (each overlap is called a stereomodel). This allows two models to be connected longitudinally by transfer points and the strips to be assembled for stereo restitution. An adjacent strip usually overlaps laterally by 20–30 per cent to cover a photogrammetric block in a survey area. Recent improvements to aerial survey flights entail determination of the exposure station co-ordinates (x'_o, y'_o, z'_o) via airborne differential GPS. Furthermore, image motion compensation allows the shift of the image plane by an amount commensurate with the aircraft speed, so that long exposures (1/100th second) are possible on high-resolution, low-sensitive film with 60 lp/mm. A prerequisite is that the camera is carried in a gyro-stabilized mounting, so that changes in the aircraft's attitude do not affect the long exposure. GPS navigation allows us to restrict the overlap conditions to a very small limit (e.g. 10–15%). It also allows control of the location of adjacent models from strip to strip (see, for example, Hartfield, 1997).

Aerial photography is restricted by film sensitivity to the visual and near-infrared electromagnetic spectrum. Black and white aerial photos usually contain images in the combined visual (400–700 nm) wavelength spectrum. Infrared images are exposed in the 500–900 nm wavelength spectrum. Colour films are three-layer films sensitive to blue (400–500 nm), green (500–600 nm), and red (600–700 nm). False-colour infrared film is sensitive to green (500–600 nm), red (600–700 nm), and infrared (800–900 nm), which becomes blue, green, and red on development. Infrared film is widely used in vegetation studies and camouflage detection because of its sensitivity to infrared radiation, which reveals the status of healthy vegetation.

Scanners originated during the 1960s at the Environmental Research Institute of Michigan (ERIM) (Figure 12.6). The electro-mechanical scanner enables individual pixels from the visual to the thermal range to be exposed on an array of silicon diodes, on to which a ray is optically separated by diffraction. The Landsat Thematic Mapper, with its seven spectral channels, is a good example of such a scanner with 30-m ground pixels. Airborne scanners, such as Daedalus with eleven channels, also belong to this category.

electro-mechanical scanner
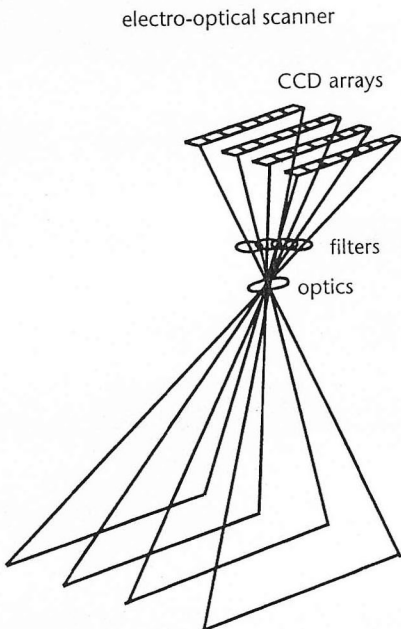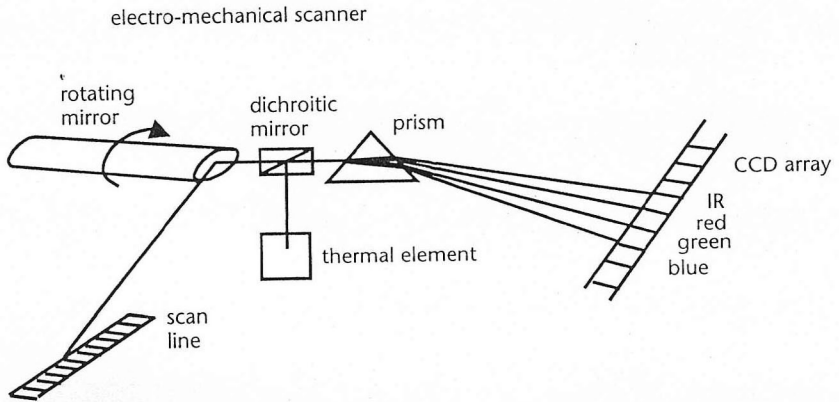

electro-optical scanner

FIGURE 12.6 Electro-mechanical and electro-optical scanners.

Electro-optical scanners used in the *Système probatoire de l'observation de la terre* (SPOT), for example, enable us to record different images in specific spectral channels by optical projection on to a linear array perpendicular to the flight path. If several arrays are filtered, these can be combined to colour or false-colour digital images at 20-m ground pixels. The multi-spectral images can be merged by image processing with 10-m ground pixels using a single, double-resolution, panchromatic channel of the same area. Charged coupled device (CCD) arrays are sensitive to the visible and near-infrared regions of the electromagnetic spectrum, but not to the thermal infrared bands.

More recently, radar sensors have been developed primarily because of their promise of good quality images under conditions in which optical sensors are not effective, for example through cloud cover.

As the solar (passive) radiation is generally too weak in the microwave range, microwave remote sensing is carried out by radar systems generating their own energy. The energy has a wavelength of a few centimetres (X-band = 3 cm). It is transmitted from an antenna in short, successive pulses. The antenna is switched alternately from transmission to reception, permitting reception of backscattering pulses from the terrain points. The pulse duration determines the resolution in range direction, while the time difference between transmission of the pulse and reception of the backscattered signal, with a known velocity of electromagnetic wave propagation, yields the double distance between the antenna and terrain point.

Brute force radar systems (SLAR) only use the time information. The greater the length of the antenna, the narrower the antenna beam becomes, and the more it approximates a plane. Since long antennas are impractical because of energy and space constraints in aircraft and satellites, coherent radar systems (synthetic aperture radar (SAR)) are preferred. They constitute the current standard.

Aircraft are still a significant platform for sensors, complementary to satellites. An aeroplane makes possible a systematic coverage of the terrain with regular overlap conditions and restitution of the images into 3D terrain information by means of photogrammetry. Flight plans can be executed accurately with modern navigation systems (GPS). The aeroplane carries the survey camera in a mounting and the camera lens points towards the terrain at a near-vertical direction through a camera window. The flying altitude depends on the type of aeroplane used: simple, motor-driven aeroplanes can reach an altitude of up to 5 km with oxygen support for the crew, while pressure-cabin aircraft with jet engines can fly at a height of 12 km, and supersonic aircraft at 20 km or more. The aeroplane velocity sets the lower limits of flights, since it must be possible to meet the repeat cycle of successive exposures necessary to achieve the longitudinal overlaps. Thus, image scales from about 1 : 3,000 to 1 : 130,000 can be achieved with aerial surveys.

Satellite platforms have existed since the launch of Sputnik by the former USSR in 1957. A few years later, Russian and US satellites were carrying imaging sensors. Nowadays, satellite-imaging systems are operated by many

national and international space agencies in the USA, Japan, Russia, India, France, Germany, China, and Canada.

The orbit of a satellite depends on its height above the terrain. Geostationary orbits operate in an equatorial plane at a height of 37,000 km. They rotate once per day in synchrony with the Earth and appear to stay in a fixed position relative to the Earth. Geostationary orbits are ideal for communication satellites and for weather satellites (Meteosat, GOES, GMS, Insat). Earth observation satellites (Landsat, SPOT) operate at lower heights of 400–800 km and these rotate around the Earth in about 90 minutes. A sun-synchronous orbit is generally chosen, so that each equator crossing always takes place at the same time of the day (e.g. at 10.30 a.m.).

Depending on the swath width of the sensor, repetition rates for the same area can be achieved from 12 hours (NOAA) to 17 days (Landsat) to 28 days (SPOT). Cloud cover restrictions for optical sensors often do not permit cloud-free images to be obtained (for NOAA satellites, a global coverage can be obtained in 15 days). In temperate zones, optical remote sensing satellites mostly do not permit images of the same area to be repeated in less than three months. Satellites with radar systems (ERS, Radarsat, JERS) do not have such restrictions. The prerequisite is that the imaged pixels can be transmitted at a sufficiently high rate (at least 100 Mb/s). This is best achieved by locating receiving stations around the world, unless temporary on-board storage is provided.

Orbiting laboratories, such as Space Shuttle or MIR, have orbital heights between 200 km and 400 km above the Earth. Their images must take variations of the sun's angle into account. The potential for achieving a global coverage is summarized in Figure 12.7. A summary of recent and upcoming high-resolution missions is shown in Table 12.1. Figure 12.8 shows a high-resolution image produced by a Russian KVR 1000 camera at 2-m pixels (DD5).

12.5 Vector data acquisition by map digitizing and photogrammetry

Digital vector data can be obtained most easily and cheaply by vector digitization of existing maps. Manual digitizers vectorize successive positions of the cursor, at regular distance intervals, while the cursor is moved over the tablet on to which the map is projected. Digitization of maps can be achieved much faster when the map is scanned in a raster scanner. The lines are converted into binary pixels (black or white) using thresholds. A subsequent automatic or interactive raster-to-vector conversion program can derive vectors for the black pixel sequences of the scanned map. More expensive map scanners can do this by colour separation using filters. Map digitization is only useful if the maps are reasonably up to date.

The United Nations Secretariat conducts official surveys of the world's map inventory and updates it regularly. The latest survey, conducted in 1993, on the
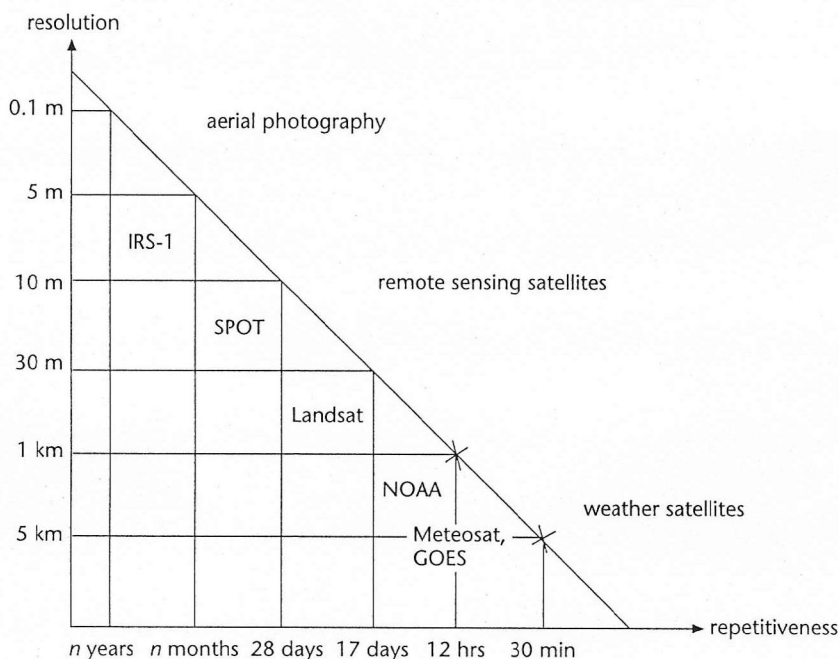
FIGURE 12.7 Resolution and repetitiveness of remote sensing missions.

status of mapping in the world is shown in Table 12.2. Table 12.3 shows the annual update rate of these maps. One-third of the Earth's land areas are mapped at a scale of 1 : 25,000, approximately 65 per cent at 1 : 50,000, and 95 per cent at 1 : 200,000. The average age of the 1 : 25,000 maps is 20 years, the 1 : 50,000 maps are nearly 50 years old, and the 1 : 200,000 maps are 30 years old. There are no figures available for maps at larger scales (e.g. for urban areas).

Analogue maps in the scales of 1 : 50,000 have, in almost all instances, been produced by photogrammetry. They have been the source for the map scales at 1 : 100,000 and smaller. In nearly all cases these maps have been digitized and thus formed the basis for geospatial information systems of the world at small and medium scales. A fully digital, global coverage is only available in the form of the 'Digital Chart of the World' at the scale of 1 : 1,000,000, published by NIMA, USA. A digital map of the world at the scale 1 : 250,000 is now in preparation. Germany is currently the only country to have full 1 : 25,000 digital coverage in the form of the ATKIS data model. Most other countries are still in the process of data conversion.

The production of maps was originally carried out by plane tabling, and other ground survey methods. In Germany, for example, this process took nearly 100 years and was completed around 1930. Plane tabling was cumbersome and costly, and this led in the late 1930s to photogrammetric stereoplotting becoming the standard mapping method throughout the world. The bulk

TABLE 12.1 High-resolution missions

Sensor	Pixel size	Mission	Year
Cameras by RKA (Russia)			
KFA 1000	5 m	MIR & KOSMOS	1988
KFA 3000	5 m	MIR & KOSMOS	1990
KVR 1000	2 m	MIR	1992
KVR 1000	2 m	SPIN-2 TM	Feb 1998
Stereo Line Scanner by DLR (Germany)			
MOMS 02-D	4.5 m (15 m)	Space Shuttle	1993
MOMS 02-P	6 m (18 m)	MIR-PRIRODA	1996–98
Scanners by ISRO (India)			
IRS 1C	6 m	IRS 1-C	1997
Commercial scanners (in preparation)			
IKONOS 1	1 m (4 m)	Space Imaging	Fall 1999
ORBVIEW 3	1 m (4 m)	Orbimage	2000
Quick Bird	1 m	EarthWatch	2000
EROS B	1 m	West Indian Space	2000

of the work was carried out after the Second World War with analogue stereo-plotters. With these instruments the spatial 3D orientation of two overlapping aerial photographs can be accomplished manually. The resulting model can be viewed by means of anaglyphs or stereoscopes.

Helava invented analytical plotters in 1957, which were capable of recording model and image co-ordinates with limits of 3–5 μm with reference to the rest of the image, while a point may be visually recognized with a precision of ±5 μm. Analytical plotters, like analogue plotters, are capable of recording vector information. They are one of the means of generating vector information in a stereomodel.

On-screen monoplotting is a technique for obtaining vector data from a geometrically correct photo (orthophoto) on the computer screen. Thus, digital orthophotos may be used for updates of existing digital vector databases, which are superimposed on the digital ortho-image.

Updating of digital databases via workstations is also possible in stereo, using digital stereo workstations. A digital stereo workstation generates corresponding images on the display screen at sequential intervals of 50 msec each. These are displayed as polarized images that can be viewed with polarization filters or 'electronic shutters', achieved by the 'Crystal Eyes' principle in stereo.[1]

---

[1] A pair of stereo images is viewed using spectacles permitting switching of the 50-msec images on the screen alternatively to the left and right eyes, in synchronization with the screen. If the switching of the two images is faster than 15 Hz the human operator sees the images in stereo.
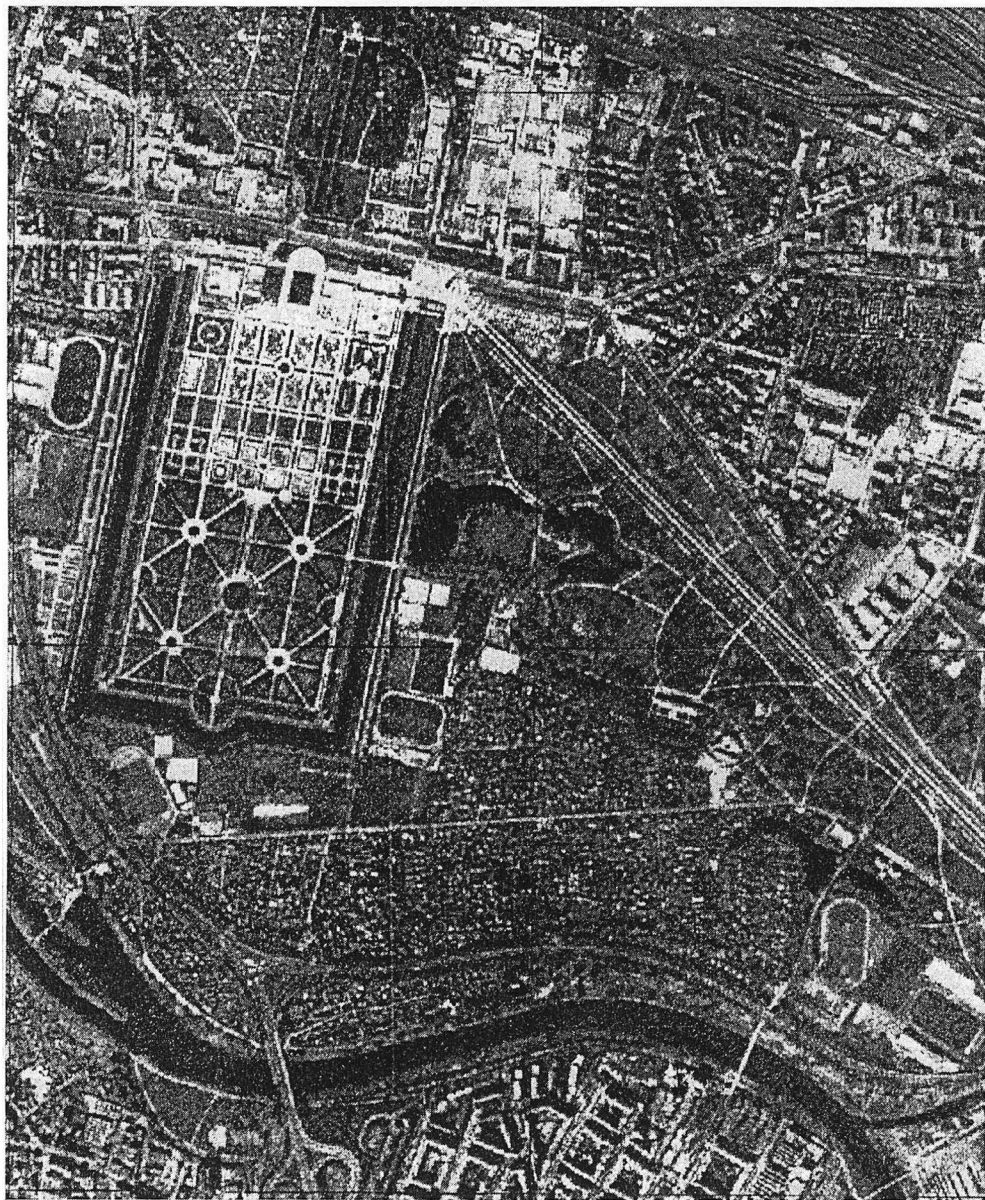
FIGURE 12.8 KVR 1000 (DD5) image of Hanover.

TABLE 12.2 Status of mapping in the world (1993), in percentage of area covered

Region	1 : 25,000	1 : 50,000	1 : 100,000	1 : 200,000
	%	%	%	%
Africa	2.9	41.1	21.7	89.1
Asia	15.2	84	66.4	100
Australia and Oceania	18.3	24.3	54.4	100
Europe	86.9	96.2	87.5	90.9
Former USSR	100	100	100	100
North America	45.1	77.7	37.3	99.2
South America	7	33	57.9	84.4
World	33.5	65.6	55.7	95.1

TABLE 12.3 Annual update rate of maps

Region	1 : 25,000	1 : 50,000	1 : 100,000	1 : 200,000
	%	%	%	%
Africa	2	2.5	4.1	1.2
Asia	4	0.8	0	2.2
Australia and Oceania	2.2	1.8	0.1	0.5
Europe	7.5	6.4	7	8.3
North America	4.8	3.1	0	6.3
South America	0	0.8	0	0.4
World	5	2.1	0.7	3.3

A stereo workstation is programmed using software corresponding to the analytical plotter principles (see, for example, Gruen, 1997, and Petrie, 1997).

12.6 Raster data acquisition by photogrammetry

Aerial photographic negatives or diapositives can be raster scanned by special scanning devices such as the SCAI scanner made by Zeiss/Intergraph, the Leica scanner, or the Wehrli scanner Rastermaster RS1. The scan raster can be as small as 7 μm (or 7.5 μm, or 12 μm). The SCAI scanner and the Leica scanner enable a whole roll of film to be digitized in an automated operation, but only the RS1 can digitize from cut film. After the digital conversion of grey level information in the film to picture elements (pixels), the raster image can be subjected to all the facilities of digital image processing such as rectification to produce an orthophoto image. Digital image processing allows us to geometrically distort or rectify the image (see, for example, Lee and Thorpe, 1997).

The collinearity equations of Figure 12.2 are functions valid for aerial pho-

tographs. A pixel x_i, y_i is chosen (together with an appropriate height z_i from a digital terrain model) to calculate the corresponding image point x'_i y'_i whose grey level d_i is transferred to the output pixel (orthophoto pixel). There are a variety of computational techniques which improve these transformations. Depending on the distortions of the imagery (e.g. Landsat), the collinearity equations may be replaced by a simpler function, such as a second-degree polynomial:

$$x'_i = a_o + a_1x_i + a_2y_i + a_3xy + a_4x^2$$
$$y'_i = b_o + b_1x_i + b_2y_i + b_3xy + b_3y^2$$

with the coefficients to be calculated from control points and their identified image points. Each sensor type (SPOT, Radar, etc.) accordingly has its own rectification function. The resultant ortho-image corresponds to the required geometry of a GIS referenced to a specific datum on a reference ellipsoid (such as WGS84 on ITRF) and a chosen map projection (e.g. UTM or 3° Transverse Mercator). As elevations are usually based on the geoid as a vertical reference, a conversion for standard orthometric heights to ellipsoidal heights on the basis of our knowledge of geoidal undulations is required (see Chapter 11).

12.7 Digital elevation models by photogrammetry

A digital elevation model (DEM) usually consists of a rectangular grid based on a reference system and a specific map projection (e.g. UTM or 3° Transverse Mercator). For the grid points the elevation is recorded as an attribute.

When photogrammetric map manuscripts or topographic maps are available, the elevation distribution of the terrain is usually depicted by contour lines. In analogue stereoplotters, the operator follows lines of equal elevation, the contours. Recording devices may register them directly in digital vector form. The digitized contours may be used to interpolate elevations at the grid points. A variety of interpolation models has been used for this purpose, resulting in a variety of DEM interpolation programs. This method introduces distortions in the terrain model because the linear interpolation between contours ignores bumps and breaks in the terrain that fall within the contour interval. More sophisticated models allow for the introduction of breaklines in a discontinuous terrain as required in highway construction or terrain modelling in mountainous areas. No smoothing takes place over such breaklines, thus providing a more truthful rendition of the terrain.

In analytical plotters or in digital workstations, the sequence of regular grid points may also be precalculated and set in a stereomodel for operator measurement of the height by stereo observation. Such an interactive method has the advantage of being able to eliminate ground points which are hidden by houses or trees.

Since operator measurement of contours or of regular grids is a cumbersome and time-consuming operation, attempts have been made to determine heights automatically by digital image correlation (also called image

matching). The principle of image matching is based on calculation of the correlation coefficient for two matrices of pixels of a reference image and that of the corresponding stereo pair image. The promise of this technique can be illustrated as follows.

Standard topographic maps usually show only ground elevations, but not building heights. New requirements by the telecommunications industry have raised the need for the creation of 3D city models by rapid means. While semantic modelling techniques to extract features such as houses, roads, and other objects automatically are still at the research stage and not yet available for operational use, some progress has been made in generating 3D city models by a combination of technologies. For example, a vector-based GIS may allow areas of existing buildings to be predefined in 2D (see Figure 12.9), and only those areas are then selected for 'brute force' digital image correlation methods to determine automatically the missing heights of the buildings in comparison to the ground heights contained in the GIS (see Figure 12.10). Oblique views of the schematic building distribution of a city thus become possible in an effective manner via ray tracing algorithms (see, for example, Ackermann, 1997, and Lang and Foerstner, 1996).

The computation of digital elevation models by SAR interferometry is now being tested and further explored. The technique follows the principle of computing an interferogram on the basis of phase difference information of two radar signals emanating from two different locations separated by a known distance, the base.

The main problem with radar interferometry from two different orbits (or satellites) is that the length and the orientation of the base are not well known. Thus, the antenna positions must be estimated from orbital data resulting in ambiguities in the results. At the same time, multiple reflections, radar shadows, and foreshortening disturb the interferometric fringes from which the computations are made.

Current radar systems, such as ERS-1, ERS-2, JERS 1, Radarsat, and a combination of ERS-1 and ERS-2 when flown in a one-day sequence as a tandem mission, lead to interference ambiguity problems, yielding accuracies of ±15 m for a 100–300 m base line in rather flat areas without vegetation, with discrepancies of up to 100 m in mountainous and forested areas. The longer the base line, the more noise that is expected in the interferometric signals, which ultimately limits the achievable accuracy. On the other hand, a short base length of less than 100 m diminishes the geometric accuracy; unfortunately, such a digital elevation model is not very useful.

When two interferograms are used as difference interferograms, however, in the form of 'differential interferometry', the result is useful for detecting surface elevation changes of a few millimetres or centimetres, e.g. in ice movements, plant growth, or volcanic activity. It is hoped that the Shuttle Topographic Radar Mission will bring improvements in the near future. Two separate radar systems are to be mounted on a beam that can be extended up to 60 m. The accurate position of the two radar systems will be monitored by

Cologne Buildings
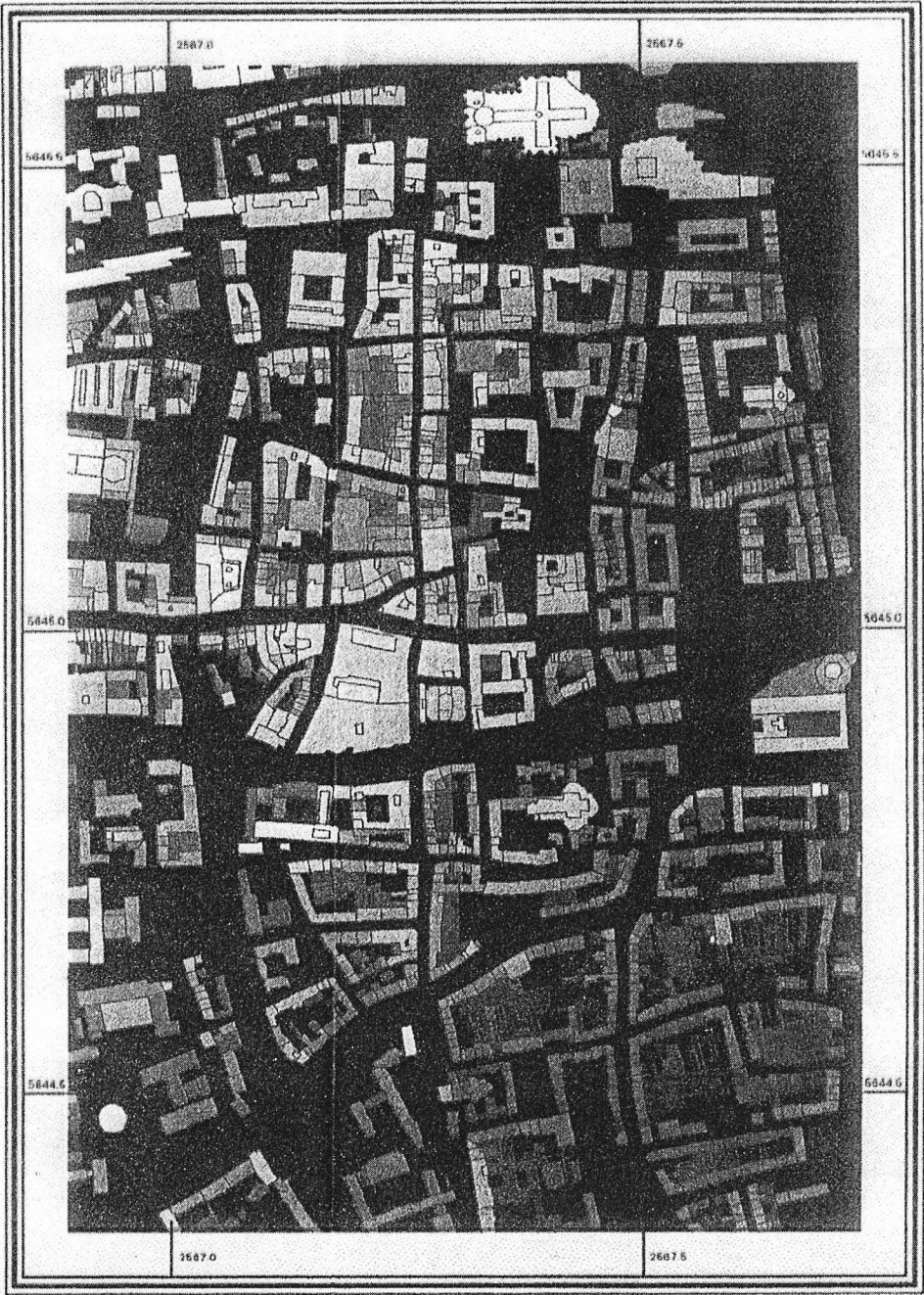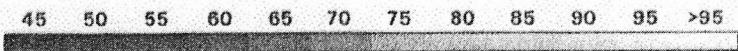
Scale 1 : 6.000

Height (m. above NN):

45   50   55   60   65   70   75   80   85   90   95   >95

FIGURE 12.9 GIS extracted buildings.

FIGURE 12.10 Image correlation results for buildings.

differential GPS, and the base length will be measured within a few millimetres by laser techniques. This may bring the expected accuracy of digital elevation models down to ±5 m. Within a 10-day shuttle mission, a significant part of the land mass could be covered by interferograms, offering an economic measurement capability for digital elevation models.

12.8 Thematic data acquisition by remote sensing

Thematic data are best collected for specific object classes (roads, forest areas, agricultural crop areas, settlement areas, etc.). Objects are defined by their boundaries with the possibility of forming subclasses with sub-boundaries, all arranged in a topologically structured manner. For objects for which boundaries have been graphically defined and identified by unique numbers, thematic information becomes an attribute in a relational database (e.g. in ESRI's Arc/Info or in Intergraph's MGE or MGA). Such object attributes can be derived by visual image interpretation from multi-spectral (colour/ false colour) and textural signatures. Context information may aid in the interpretation.

Multi-spectral and multi-temporal image classification may be automated by statistical analysis. After geometric co-registration of the images, the pixels of corresponding geometry in both images are recorded in a multi-dimensional space, as shown in Figure 12.11 for a 2D example. Images of water pixels will show low reflections in all spectral channels; they will all be accumulated in the lower left corner of the diagram. Coniferous forest will show low reflections in the green spectrum, but due to the water-filled cell structure of vegetation it will
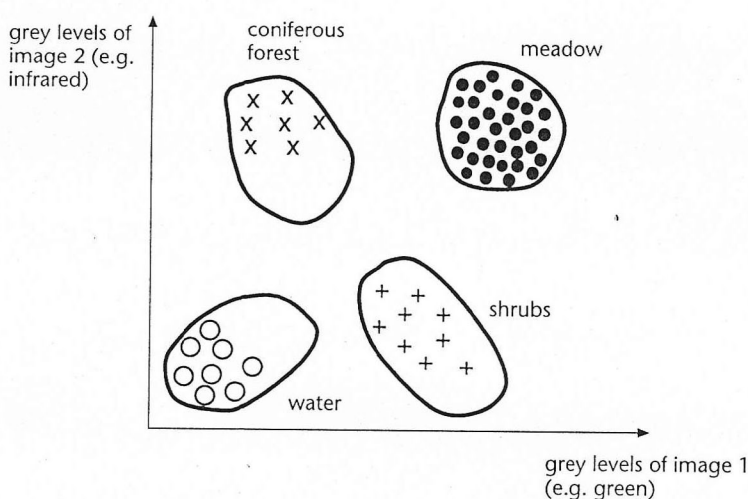

FIGURE 12.11 Automatic image classification.

show a high reflectance in the infrared, shown in the upper left corner of the diagram. Low infrared but high green levels will indicate dry shrubs.

In the sampled space, statistical boundaries between clusters must be found to distinguish the four classes shown in the example. This is done most easily by probability ellipses around the class clusters in the 2D example shown. Any pixel not falling into the cluster ellipses is shown as a fifth category of 'other classes'. Landsat™ enables hyper-ellipsoids to be generated in seven dimensions for the seven spectral channels available. The number of dimensions may be expanded to fourteen when two multi-temporal images are available at different time intervals.

The classification algorithm becomes very computation intensive if all fourteen channels are used. It is therefore better to reduce the number of channels by making a principal component analysis, in which only the most significant components of the hyper-ellipsoids are used for classification, thus reducing the information to low-correlation principal components. More independent object classes may thus be differentiated.

Under certain circumstances, knowledge-based systems can be applied and semantic networks may be utilized in automatic verification of object classes. They may be used to monitor changes in geometry and classification of objects, in particular. If an object has been defined by geometry and attributes in an existing GIS, then new images of the object may be geometrically superimposed on to the database. The spectral content and the texture properties of the imaged object may be verified using a hypothesis that the object still agrees with the original classification in content and geometry. This allows a method to be set up for automatic change detection (see Figure 12.12).

12.9 Cadastral photogrammetry

The cadastre consists of a geometric description of land parcels and attribute information concerning ownership or user rights. Depending on the local situation, other data, such as land use, soil quality, occupancy, mortgages, or other encumbrances may also be included. Parcels of land referenced to a consistent co-ordinate system are a natural entity for holding attribute values necessary when the spatial distribution of these attributes needs to be part of decision-making or civic consultation processes.

Early attempts to establish cadastral records by photogrammetry resulted in signalization of boundary monuments, if these were available. Large-scale (1 : 1,000 or 1 : 2,500) aerial surveys permitted the determination of the co-ordinates of the signals with an accuracy of a few centimetres. Only in rare cases, where fences, walls, or hedges mark the occupation limits of the parcels is direct mapping via photogrammetric plotters possible. Orthophoto mapping technology (particularly the digital orthophoto) offers new possibilities for reaching an economic solution for determining cadastral boundaries, but then adjudication of boundaries using photography or orthophotography in the field becomes necessary. The boundary points are marked on copies of the

Semantic Modelling

Example: Verification of ATKIS Forest Objects

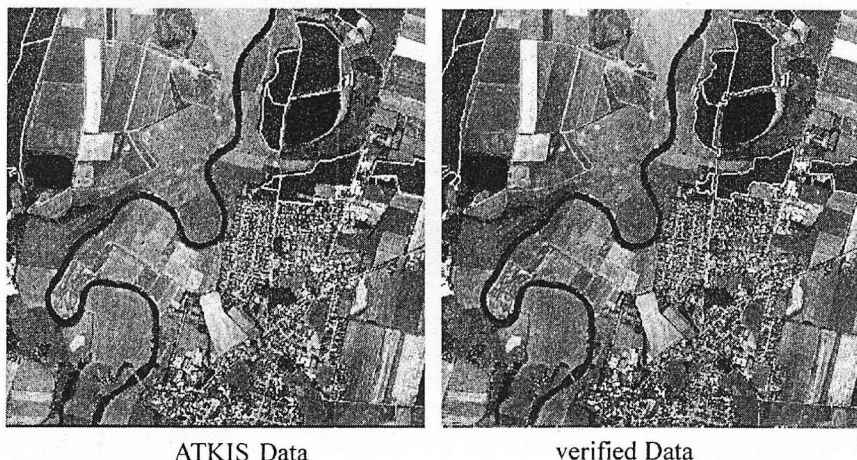ATKIS Data   verified Data

FIGURE 12.12 Automatic change detection.

photo or orthophoto. The neighbours of each parcel agree on this document by signing it on the location of the identified boundary point.

In some developing countries, where there may be large parcels, high-resolution satellite images offer possibilities for a quick and economic solution for establishing a 'graphical cadastre' for public or even for private purposes.

12.10 Cost considerations

Remote sensing and survey costs depend on map scale or resolution. Table 12.4 gives a summary of the costs per square kilometre for various German technical co-operation projects. The costs include acquisition of imagery, image processing and interpretation, as well as the required ground data supplementation and the preparation of a final product. Surveys at scales of 1 : 50,000 or smaller may utilize current satellite imagery at an image data cost of less than US$1/km². Larger scale survey costs depend on the photo scale and cost between US$4/km² (1 : 80,000) and US$40/km² (1 : 4,000) on average. In general, project costs are one to two orders of magnitude higher than imagery costs. Vector mapping costs, requiring supplementary ground data acquisition, are the most expensive item. By comparison, orthophoto mapping leads to more reasonable costs. The requirements of global GIS at the scale of 1 : 200,000 can generally be met for a cost of less than US$10/km² using satellite

TABLE 12.4 Summary of costs for technical co-operation projects

Field	Type	Scale	Imagery	Cost (US$/km^2)
Agriculture	Phenol. change	1 : 1,000,000	NOAA	80
Bio-material	Biomass change	1 : 1,000,000	NOAA	80
Forestry	Forest mapping	1 : 250,000	MSS	6
Geology	Reconnaissance	1 : 100,000	TM	20
Forestry	Forest development	1 : 100,000	TM	20
Irrigation	Watershed mapping	1 : 100,000	TM	10
Regional planning	Planning study	1 : 100,000	TM	25
Land use	Land use mapping	1 : 100,000	TM	13
Bio-material	Biomass inventory	1 : 100,000	TM	20
Erosion	Vegetation cover	1 : 100,000	TM	20
Desertification	Change detection	1 : 100,000	TM	35
Food security	Cultivation inventory	1 : 100,000	TM	25
Environment	Environment inventory	1 : 100,000	TM	50
Regional planning	Feasibility study	1 : 50,000	Spot-XS	40
Environment	Risk zone mapping	1 : 50,000	KFA 1000	150
Urban development	Urban change	1 : 50,000	KFA 1000, Spot-P	45
Topography	Base map	1 : 50,000	aerial photo	120
Geology	Photogeology	1 : 25,000	aerial photo	50
Transport	Road design	1 : 20,000	aerial photo	180
Topography	Orthophoto	1 : 12,000	aerial photo	24
Water supply	Base map	1 : 10,000	aerial photo	800
Forestry	Forest inventory	1 : 10,000	aerial photo	350
Land use	Land use mapping	1 : 10,000	aerial photo	520
Bio-material	Energy study	1 : 10,000	aerial photo	250
Transport	Photogr. map	1 : 10,000	aerial photo	700
Cadastre	Orthophoto map	1 : 10,000	aerial photo	400
Topography	Base map	1 : 5,000	aerial photo	2,000
Topography	Orthophoto	1 : 5,000	aerial photo	78
Cadastre	Photogr. or survey map	1 : 2,000	aerial photo	10,000
Cadastre	Orthophoto	1 : 2,000	aerial photo	1,000
Topography	Orthophoto	1 : 1,000	aerial photo	800
Urban cadastre	Base map	1 : 1,000	aerial photo	20,000
Urban cadastre	Multi-purpose cadastre, utilities, topography	1 : 500	aerial photo	40,000

TABLE 12.5 Prices of digital map data (Lower Saxony, Germany)

Map data	US$/km^2
Raster-scanned maps	
1 : 500,000	0.01
1 : 100,000	0.15
1 : 50,000	0.60
1 : 25,000	2.50
1 : 5,000	30
Vector data	
1 : 10,000	35
1 : 1,000	1,000
Digital elevation models	
1 : 50,000	2
1 : 5,000	65
Digital orthophotos	
1 : 10,000	30
1 : 5,000	80
1 : 1,000	800

images. The requirements of regional GIS at a scale of 1 : 50,000 will cost about US$100/km^2 on average, whereas local GIS at scales between 1 : 1,000 to 1 : 10,000 will cost between US$1,000–10,000/km^2, unless orthophoto mapping is used at between US$30–800/km^2.

Surveys and mapping administrations are beginning to market their base products. Table 12.5 lists the current prices of the state survey authority of Lower Saxony in Germany.

12.11 Conclusion

One of the reasons for including a description of several classical techniques of photogrammetry in this book is because much topographic source data used in the GDI environment depends on topographic maps constructed using these techniques. Modern remote sensing and photogrammetry offer a wide variety of new methods for geospatial data acquisition. Improvement in the precision and cost-performance continue to be made: in airborne methods by the forward-motion compensation in cameras, and in satellite platforms by the application of increasingly higher resolutions. By far the most significant development in terms of cost and quality performance is the integration of differential GPS techniques (see Chapter 11, pp. 183–5) with 'sensing' processes. As can be seen from the cost-performance figures, the optimization

of technical choices is important and has ongoing consequences for the budgets, and consequently for the ultimate cost of the GDI.

The optimization process requires specialized expertise which developers of GDI must have at their disposal to ensure that the right choices are made for the purposes identified. More recently, military high-resolution remote sensing technology has been released for commercial exploitation by the private sector in the USA. As a result, several corporations have emerged with plans to provide a complete suite of commercial data acquisition services, including value-added product services partly based on these new facilities. The pricing structures of these services are still unclear but it is hoped that healthy competition will bring them down to interesting levels (see, for example, Li, 1998). Aside from the impact these commercial services may have on national surveying and mapping agencies, it will be interesting to watch this development closely for other jurisdictions.

Bibliography

ACKERMANN, F. (1997). 'Digital Terrain Models—New Techniques, Demands, Concepts', IAPRS Commission 3/4 Workshop, 32: 3–4W2, Stuttgart.

DANGERMOND, J. (1997). 'Synergy of Photogrammetry, Remote Sensing, and GIS', Photogrammetric Week '97, Stuttgart: Heidelberg, Wichmann, pp. xi–xvi.

GRUEN, A. (1997). 'Digital Photogrammetric Stations Revisited: A short list of unmatched expectations', *Geomatics Information Magazine* (GIM) January, pp. 20–7.

HARTFIELD, P. (1997). 'Higher Performance with Automated Aerial Triangulation', Photogrammetric Week '97, Stuttgart.

LANG, F. and FOERSTNER, W. (1996). '3D-city modelling with a digital one-eye-stereo system', IAPRS, 31/4: Vienna.

—— (1996). 'Surface reconstruction of man-made objects using polymorphic mid-level features and generic scene knowledge', IAPRS, 31/B3 Commission 3: Vienna.

LEE, G. and THORPE, J. (1997). 'USA's National Digital Orthophoto Program', Photogrammetric Week '97, Stuttgart.

LI, R. (1998). 'Potential of High-resolution Satellite Imagery for National Mapping Products', *Journal of Photogrammetric Engineering and Remote Sensing*, 64/12: pp. 1165–9.

PETRIE, G. (1997). 'Digital Photogrammetric Workstations: A perspective on suppliers and users'. *Geomatics Information Magazine* (GIM) July, pp. 18–23.